Optimum Sparse Subarray Design for Multitask Receivers

ANASTASIOS DELIGIANNIS, Member, IEEE
Loughborough University, Loughborough, U.K.

MOENESS AMIN, Fellow, IEEE
Villanova University, Villanova, USA

SANGARAPILLAI LAMBOTHARAN, Senior Member, IEEE
Loughborough University, Loughborough, U.K.

GIUSEPPE FABRIZIO, Fellow, IEEE
Defence Science and Technology Group, Edinburgh, Australia

The problem of optimum sparse array configuration to maximize the beamformer output signal-to-interference plus noise ratio (MaxSINR) in the presence of multiple sources of interest (SOI) has been recently addressed in the literature. In this paper, we consider a shared aperture system where optimum sparse subarrays are allocated to individual SOIs and collectively span the entire full array receiver aperture. Each subarray may have its own antenna type and can comprise a different number of antennas. The optimum joint sparse subarray design for shared aperture based on maximizing the sum of the subarray beamformer SINRs is considered with and without SINR threshold constraints. We utilize Taylor series approximation and sequential convex programming techniques to render the initial nonconvex optimization a convex problem. The simulation results validate the shared aperture design solutions for MaxSINR for both cases where the number of sparse subarray antennas is predefined or left to constitute an optimization variable.

Manuscript received January 3, 2018; revised June 3, 2018; released for publication July 26, 2018. Date of publication August 27, 2018; date of current version April 11, 2019.

DOI. No. 10.1109/TAES.2018.2867258

Refereeing of this contribution was handled by F. Gini.

The work of A. Deligiannis and S. Lambotharan was supported by the Engineering and Physical Sciences Research Council under Grant EP/K014307/1 and the MOD University Defence Research Collaboration in signal processing. The work of Dr. Amin was supported by NSF Grant 1547420 and by the 2017 Fulbright Scholarship program.

Authors' addresses: A. Deligiannis and S. Lambotharan are with the Wolfson School of Mechanical, Manufacturing and Electrical Engineering, Loughborough University, Loughborough LE11 3TU, U.K. E-mail: (A.Deligiannis@lboro.ac.uk, S.Lambotharan@lboro.ac.uk); M. Amin is with the Center for Advanced Communications, Villanova University, Villanova, PA 19085 USA, E-mail: (moeness.amin@villanova.edu); G. Fabrizio is with the Defence Science and Technology Group, Edinburgh, SA 5111, Australia E-mail: (joe.fabrizio@dsto.defence.gov.au). *(Corresponding author: Anastasios Deligiannis.)*

I. INTRODUCTION

Shared aperture antenna describes a system of two or more sparse subarrays, each performing a separate task, deployed on a common aperture [1]. The subarray tasks are dependent on the system operation, which could jointly support several required services. A three-dimensional shared aperture antenna that supports different operating frequencies was proposed in [1]. The compound system consists of two stacked arrays, transmitting through the same aperture, the upper level operating in the L-band and being electrically isolated from the lower one that operates in the X-band. The coexistence of radar, electronic warfare, and communications functions on the same aperture was investigated in [2], where subarrays with different operating frequencies and polarization are utilized to perform separate tasks. The design of a shared dual-band transmitting/receiving platform, where separated sparse subarrays of S-band and X-band elements are designed for simultaneous transmitting and receiving operation was investigated in [3]. Three different radar applications of a shared aperture antenna using interleaved sparse subarrays on a common platform were considered in [4], namely, multifrequency shared aperture antenna, shared aperture antenna implementing polarization agility, and interleaved transmitting/receiving shared aperture antenna. The synthesis of linear multibeam arrays on a shared aperture through hierarchical almost difference set based interleaving was studied in [5].

In this paper, each sparse subarray of the shared aperture performs separate beamforming and strives to maximize the signal-to-interference and noise ratio (SINR) for its designated source or for a specific direction. Maximizing SINR at the receiver increases the probability of target detection in radar and reduces bit error rates in communications. In this respect, the different tasks assigned to the shared aperture antenna could belong to the same functionality, i.e., either radar or communication across different functions as part of platform coexistence, i.e., joint radar communication system [6]. In either case, the system may mandate unshared antennas among the subarrays to reduce signal processing complexity and limit radar cross sections. Moreover, the different tasks may demand antennas with diverse properties, polarization or bandwidth [3]. The beamformer output is not only affected by the antenna output multiplicative coefficients but also by the antenna array configuration [7]–[9]. Hence, optimal beamforming should utilize both the beampattern array coefficients as well as the array configuration [10], [11].

Optimal beamforming techniques efficiently mitigate the interference and noise at the output of the system while enhancing the response toward the sources of interest (SOI) [12]–[16], casting it as a powerful tool for many active and passive sensing applications, such as radar, sonar, wireless communications, radio telescope, ultrasound, and seismology [17]–[21]. Sparse transmit array design for radiating shaped beamformers was investigated in [22] exploiting compressive sensing. Adaptive interference

nulling techniques based on the appropriate selection of the array elements were proposed in [23] and [24], utilizing genetic algorithms and SINR maximization, respectively. As demonstrated in [25] and [26], sparse array configuration has a substantial impact on both the beamformer output signal-to-noise ratio (SNR) and SINR. Optimum adaptive sparse arrays for maximizing SNR (MaxSNR) and SINR (MaxSINR) are superior to structured sparse arrays such as coprime, nested, and uniform arrays [26]. This is attributed to the fact that adaptive beamforming and sparse array design take into consideration the operating environment, by incorporating the source, interference, and noise spatial and temporal characteristics in the optimization [27].

Most of the existing work on maxSINR beamforming focuses on a single mission array where the entire array aperture, regardless of whether it is full or sparse, is tasked to deal with one or more sources in the field of view [28]. In such case, the main objective is to maximize the SINR at the output of the receiver by optimally configuring the array and deciding on the beamformer coefficients. This technique is deemed to result in unequal SINR or SNR for the sources considered and does not guarantee an acceptable minimum SNR or SINR performance for any of the sources. Using a separate beamformer, along with its antennas and coefficients, for each source is a generalization of the above technique.

In this paper, we investigate scenarios that fall into the aforementioned framework of multimission or multitask sensing of a shared aperture with separate, but complementing, sparse subarrays. That is, the combined subarrays make up the system aperture. The multiple sources considered are in the far field and may represent targets reflecting a transmitted waveform or active emitters, thus covering many scenarios including radar, wireless communications, electronic warfare, and radio telescope. We propose a method for optimum design of antenna aperture comprising multiple sparse subarrays, each processes the signal from one source. The goal is to select the antenna positions and coefficients to jointly maximize the SINR for all sources. The optimum subarrays are obtained by performing a joint SINR optimization for matched minimum variance distortionless response (MVDR) beamforming. We examine both cases in which specific cardinality of antennas per subarray is set *a priori* and when the number of antennas in each subarray is left as an optimization variable. By considering the cardinality as an optimization variable, we provide more design flexibility and additional degrees of freedom to the system, resulting in higher SINR performance, especially when dealing with high spatially correlated sources. The choice of SINR as a performance metric is motivated by the fact that higher SINR enhances target detection in radar, and minimizes bit error rates in communications, leading to a better quality of service [29]–[32]. We also propose a joint optimum sparse subarray design technique with the objective of maximizing the SINR of some sources, while attaining a predefined SINR threshold for the remaining sources. We utilize Taylor series approximation and sequential convex programming (SCP) techniques to render the initially nonconvex SINR optimization problems as convex.

The rest of the paper is organized as follows: The mathematical model of the system is formulated in Section II. The sparse subarray design for both cases of given number of antennas per subarray and when the cardinality of antennas is a design variable is examined in Section III. The SINR constrained optimum sparse subarray design is presented in Section IV. Simulation results and remarks on the results are given in Section V, and the final conclusions are drawn in Section VI.

II. SYSTEM MODEL

We consider a uniform linear array (ULA), consisting of N isotropic antennas with positions given by $y_n d$, $n = 1, \ldots, N$, where d denotes the interelement spacing. Suppose there are P sources impinging on the array from directions defined by $\{\phi_{s,1}, \ldots, \phi_{s,P}\}$. The main goal of this work is to jointly design P sparse, nonoverlapping subarrays that collectively span the entire length of the ULA. Depending on the assigned mission, each subarray is tasked either with communicating with a source or detecting the presence of a target along a specified direction. The number of antennas in subarray i is given by K_i, $i = 1, \ldots, P$ with coordinates specified by $y_{in}d, n = 1, \ldots, K_i$. Assume there are m interfering signals impinging on the array from angles $\{\phi_{i,1}, \ldots, \phi_{i,m}\}$. For the communications applications, all $P-1$ emitters other than the one tasked to a given subarray are considered interferences for that subarray. Depending on signal carrier and bandwidth, these interferences can be full-band or partial-band interferences. For a radar function, interference will only be present if target backscatterings are in the same range Doppler cell. An illustrative example of a setup with two sparse nonoverlapping subarrays and an interfering source is presented in Fig. 1. The receive steering vectors for subarray i toward direction ϕ can be written as

$$\mathbf{a}_i(\phi) = [e^{jk_0 y_{i1} d\cos\phi}, \ldots, e^{jk_0 y_{iK_i} d\cos\phi}]^T, \quad i = 1, \ldots, P \tag{1}$$

where k_0 is the wavenumber and is given by $k_0 = 2\pi/\lambda$ with λ denoting the wavelength. The received signals for subarray i at time instant t can be written as

$$\mathbf{x}_i(t) = s_i(t)\mathbf{a}_i(\phi_{si}) + \mathbf{C}_i\mathbf{c}_i(t) + \mathbf{n}_i(t) \tag{2}$$

where $\mathbf{C}_i = [\mathbf{a}_i(\phi_{s,1}), \ldots, \mathbf{a}_i(\phi_{s,i-1}), \mathbf{a}_i(\phi_{s,i+1}), \ldots, \mathbf{a}_i(\phi_{s,P}), \mathbf{a}_i(\phi_{i,1}), \ldots, \mathbf{a}_i(\phi_{i,m})]$ denotes the interference array manifold matrix with full column rank regarding subarray i, $i = 1, \ldots, P$. The source i signal is represented by $s_i(t) \in \mathbb{C}$, $i = 1, \ldots, P$, with corresponding power σ_{is}^2. The interfering signals for subarray i are given by the vector $\mathbf{c}_i(t) = [s_1(t), \ldots, s_{i-1}(t), s_{i+1}(t), \ldots, s_P(t), c_1(t), \ldots, c_m(t)] \in \mathbb{C}^{m+P-1}$, with covariance matrix $\mathbf{R}_{bi}$ and $\mathbf{n}_i(t) \in \mathbb{C}^{K_i}$ denotes the received Gaussian noise vector at subarray i. We presume that the noise vectors for all subarrays have common power given by σ_n^2.

The received signal at subarray i is filtered by the receive weight, or coefficient, vector of subarray i denoted as $\mathbf{w}_i \in$

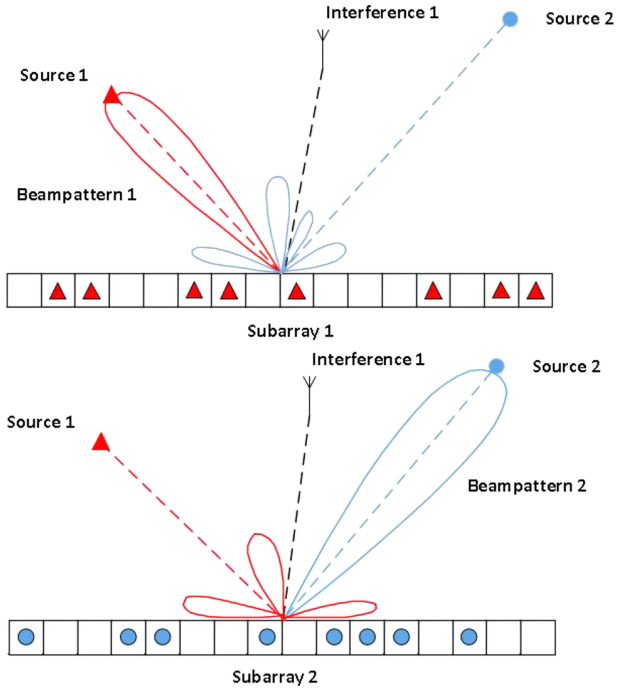

Fig. 1. Model of two separated sparse subarrays addressing two SOI in the presence of one interfering source.

$\mathbb{C}^{K_i}$. Thus, the output SINR for source i is written as

$$\text{SINR}_i = \frac{\sigma_{is}^2 |\mathbf{w}_i^H \mathbf{a}(\phi_{s,i})|^2}{\mathbf{w}_i^H \mathbf{R}_{n,i} \mathbf{w}_i} \tag{3}$$

where $\mathbf{R}_{n,i} = \mathbf{C}_i \mathbf{R}_{b,i} \mathbf{C}_i^H + \sigma_n^2 \mathbf{I}_{K_i}$ defines the interference plus noise covariance matrix for subarray i. The MVDR beamformer that maximizes the SINR, by securing the desired source signal while suppressing the undesired interference and noise, is written as [27]

$$\mathbf{w}_i = \frac{\mathbf{R}_{n,i}^{-1} \mathbf{a}(\phi_{s,i})}{\mathbf{a}(\phi_{s,i})^H \mathbf{R}_{n,i}^{-1} \mathbf{a}(\phi_{s,i})}. \tag{4}$$

By substituting (4) into (3), we obtain the output SINR of the matched MVDR beamformer at subarray i as

$$\text{SINR}_i = \sigma_{is}^2 \mathbf{G}_i = \sigma_{is}^2 \mathbf{a}(\phi_{s,i})^H \mathbf{R}_{n,i}^{-1} \mathbf{a}(\phi_{s,i}) \tag{5}$$

where

$$\mathbf{G}_i = \mathbf{a}(\phi_{s,i})^H \mathbf{R}_{n,i}^{-1} \mathbf{a}(\phi_{s,i}) \tag{6}$$

denotes the ith subarray gain of the MVDR beamformer toward the direction of source i ($\phi_{s,i}$). It is evident from (1) that the subarray configuration affects the receive steering vectors and hence, from (5), the output SINR for every subarray. To show analytically the full extent of the effect of the subarray selection on the output SINR, we utilize the matrix inversion lemma and restate the interference plus noise covariance matrix $\mathbf{R}_{n,i}^{-1}$ as

$$\mathbf{R}_{n,i}^{-1} = \sigma_n^2 [\mathbf{I}_{K_i} - \mathbf{C}_i (\mathbf{R}_{m,i} + \mathbf{C}_i^H \mathbf{C}_i)^{-1} \mathbf{C}_i^H] \tag{7}$$

where $\mathbf{R}_{m,i} = \sigma_n^2 \mathbf{R}_{b,i}^{-1}$. By defining $\text{SNR}_i = \sigma_{is}^2 / \sigma_n^2$ as the input SNR at subarray i and substituting (7) into (5), the output SINR at subarray A can be written as in (8). It is evident from (8) that the output SINR of the MVDR beamformer at subarray i is influenced by the subarray configuration through the source steering vectors $\mathbf{a}(\phi_{si})$ and the interference array manifold matrix $\mathbf{C}_i$

$$\text{SINR}_i = \text{SNR}_i [K_i - \mathbf{a}(\phi_{s,i})^H \mathbf{C}_i (\mathbf{R}_{m,i} + \mathbf{C}_i^H \mathbf{C}_i)^{-1} \mathbf{C}_i^H \mathbf{a}(\phi_{s,i})]. \tag{8}$$

III. SPARSE SUBARRAY DESIGN THROUGH SINR OPTIMIZATION

A. Given Cardinality of Antennas per Subarray

The optimum sparse subarray design can be defined as dividing the full ULA into P separate subarrays that collectively cover the entire ULA and select the optimal grid location for each subarray with the respective weights determined by MVDR beamforming. The optimum configuration of the subarrays is obtained by jointly maximizing the SINRs at the output of the different subarrays. In this section, we assume that the number of antennas that constitute each subarray is given, i.e., the values of K_i, $\forall i$ are prefixed and determined *a priori*. This number can be decided based on the achievable array gain. Hence, the main objective is to simultaneously select the optimum subarray configurations in order to maximize the SINR for each source. Toward that objective, we define P selection vectors $\mathbf{z}_i \in \{0, 1\}^N$, $i = 1, \ldots, P$, where entry "1" stands for a selected location and "0" for a discarded location for antenna placement regarding subarray i. Since we assume knowledge of all the antenna locations, we may define the full array receive steering vector toward direction ϕ as

$$\hat{\mathbf{a}}(\phi) = [e^{jk_0 y_1 d \cos\phi}, \ldots, e^{jk_0 y_N d \cos\phi}]^T. \tag{9}$$

Therefore, the respective receive steering vectors for subarray i toward angle ϕ can be given by $\mathbf{a}_i(\phi) = \mathbf{z}_i \odot \hat{\mathbf{a}}(\phi)$ and dispose of the zero entries in order to have a vector of length K_i. In order to simultaneously design the optimal sparse, separate subarrays, we consider the following joint output SINR maximization problem:

$$\begin{aligned} \max_{\mathbf{z}_1, \ldots, \mathbf{z}_P} \quad & \sum_{i=1}^{P} \text{SINR}_i \\ \text{s.t.} \quad & \mathbf{1}_N^T \mathbf{z_i} = K_i \quad \forall i \\ & \sum_{i=1}^{P} \mathbf{z}_i = \mathbf{1}_N \\ & \mathbf{z}_i \in \{0, 1\}^N \quad \forall i. \end{aligned} \tag{10}$$

The first constraint in (10) dictates the number of antennas in each subarray. The second and the third constraints ensure that the disjoint subarrays collectively span the entire ULA and that the elements of the selection vectors are strictly 0 or 1, respectively. From (5), the SINR maximization problem (10) can be restated as a subarray gain optimization problem. In particular, we can define the gain for the full ULA case by substituting (7) into (6) and replacing the subarray steering vectors with the full array steering

vectors as shown in (11), where $\hat{\mathbf{C}}_{a,i} = [\hat{\mathbf{C}}_i, \hat{\mathbf{a}}_i(\phi_{s,i})]$ and $\hat{\mathbf{C}}_i$ is defined in (12). The extended interference covariance matrix can be written as

$$\hat{\mathbf{G}}_i = \sigma_n^2[\hat{\mathbf{a}}(\phi_{s,i})^H\hat{\mathbf{a}}(\phi_{s,i}) - \hat{\mathbf{a}}(\phi_{s,i})^H\hat{\mathbf{C}}_i(\mathbf{R}_{m,i} + \hat{\mathbf{C}}_i^H\hat{\mathbf{C}}_i)^{-1}\hat{\mathbf{C}}_i^H\hat{\mathbf{a}}(\phi_{s,i})] = \sigma_n^2\frac{|\hat{\mathbf{C}}_{a,i}^H\hat{\mathbf{C}}_{a,i} + \mathbf{R}_i|}{|\hat{\mathbf{C}}_i^H\hat{\mathbf{C}}_i + \mathbf{R}_{m,i}|} \quad (11)$$

$$\hat{\mathbf{C}}_i = [\hat{\mathbf{a}}_i(\phi_{s,1}), \ldots, \hat{\mathbf{a}}_i(\phi_{s,i-1}), \hat{\mathbf{a}}_i(\phi_{s,i+1}), \ldots, \hat{\mathbf{a}}_i(\phi_{s,P}), \times \hat{\mathbf{a}}_i(\phi_{i,1}), \ldots, \hat{\mathbf{a}}_i(\phi_{i,m})]$$

$$\mathbf{R}_i = \begin{bmatrix} \mathbf{R}_{m,i} & \mathbf{0}_{1\times m} \\ \mathbf{0}_{m\times 1} & 0 \end{bmatrix}. \quad (12)$$

The equality in (11) can be proved by utilizing the block matrix determinant formula, as shown below:

$$|\hat{\mathbf{C}}_{a,i}^H\hat{\mathbf{C}}_{a,i} + \mathbf{R}_i| = \begin{vmatrix} \hat{\mathbf{C}}_i^H\hat{\mathbf{C}}_i + \mathbf{R}_{m,i} & \hat{\mathbf{C}}_i^H\hat{\mathbf{a}}(\phi_{s,i}) \\ \hat{\mathbf{a}}(\phi_{s,i})^H\hat{\mathbf{C}}_i & \hat{\mathbf{a}}(\phi_{s,i})^H\hat{\mathbf{a}}(\phi_{s,i})^H \end{vmatrix} = |\hat{\mathbf{C}}_i^H\hat{\mathbf{C}}_i + \mathbf{R}_{m,i}|\hat{\mathbf{G}}_i. \quad (13)$$

Hence, the SINR maximization (10) can be reformulated as the maximization of the logarithm of the subarray gain for each subarray as [33]

$$\begin{aligned} \max_{\mathbf{z}_1,\ldots,\mathbf{z}_P} \quad & \sum_{i=1}^{P} \log|\hat{\mathbf{C}}_{a,i}^H\mathcal{D}(\mathbf{z}_i)\hat{\mathbf{C}}_{a,i} + \mathbf{R}_i| \\ & - \log|\hat{\mathbf{C}}_i^H\mathcal{D}(\mathbf{z}_i)\hat{\mathbf{C}}_i + \mathbf{R}_{m,i}| \\ \text{s.t.} \quad & \mathbf{1}_N^T\mathbf{z}_i = K_i \quad \forall i \\ & \sum_{i=1}^{P}\mathbf{z}_i = \mathbf{1}_N \\ & \mathbf{z}_i \in \{0,1\}^N \quad \forall i \end{aligned} \quad (14)$$

where $\mathcal{D}(\mathbf{z}_i)$ denotes the diagonal matrix populated with the vector $\mathbf{z}_i$ along the diagonal. There are two reasons that render the optimization (14) nonconvex: the nonconcave objective function, that is, defined as the difference of concave functions, and the nonconvex binary constraint enforced by the antenna selection vectors $\mathbf{z}_i \in \{0,1\}^N$. However, since the objective function is the difference of concave functions, the respective global optimizer locates at the extreme points of the polyhedron and thus we may replace the binary constraint with the box constraint $0 \le \mathbf{z}_i \le 1$ [34], [35]. To circumvent the nonconcavity of the objective function, we utilize first-order Taylor series that can iteratively approximate the negative logarithms of the objective function, which cause the nonconcavity. The $(k+1)$th Taylor approximations of those terms based on the previous solution $\mathbf{z}_i^{(k)}$ are shown in (15), where $\nabla\mathbf{g}_i(\mathbf{z}_i^{(k)})$ represents the gradient of the logarithmic function $\log|\hat{\mathbf{C}}_i^H\mathcal{D}(\mathbf{z}_i)\hat{\mathbf{C}}_i + \mathbf{R}_{m,i}|$ evaluated at the point $\mathbf{z}_i^{(k)}$ and is written as in (16), where $\hat{\mathbf{a}}_{i,j}$ denotes the jth column vector of the matrix $\hat{\mathbf{C}}_i^H$. This SCP technique recasts the initially nonconvex problem to a series of convex subproblems, each of which can be optimally solved via convex optimization [36]. By substituting (15) into (14), we obtain the following approximated convex optimization problem that provides the antenna selection in the $(k+1)$th iteration based on the solution $\mathbf{z}_i^{(k)}$, $\forall i$ from the previous iteration:

$$\log|\hat{\mathbf{C}}_i^H\mathcal{D}(\mathbf{z}_i)\hat{\mathbf{C}}_i + \mathbf{R}_{m,i}| \approx \log|\hat{\mathbf{C}}_i^H\mathcal{D}(\mathbf{z}_i^k)\hat{\mathbf{C}}_i + \mathbf{R}_{m,i}| + \nabla\mathbf{g}_A^T(\mathbf{z}_i^{(k)})(\mathbf{z}_i - \mathbf{z}_i^{(k)}) \triangleq T_i \quad (15)$$

$$\nabla\,\mathbf{g}_i(\mathbf{z}_i^{(k)}) = [\hat{\mathbf{a}}_{i,j}^H(\hat{\mathbf{C}}_i^H\mathcal{D}(\mathbf{z}_i^{(k)})\hat{\mathbf{C}}_i + \mathbf{R}_{m,i})^{-1}\hat{\mathbf{a}}_{i,j},\ j = 1,\ldots,N]^T \quad (16)$$

$$\begin{aligned} \max_{\mathbf{z}_1,\ldots,\mathbf{z}_P} \quad & \sum_{i=1}^{P}\log|\hat{\mathbf{C}}_{a,i}^H\mathcal{D}(\mathbf{z}_i)\hat{\mathbf{C}}_{a,i} + \mathbf{R}_i| - T_i \\ \text{s.t.} \quad & \mathbf{1}_N^T\mathbf{z}_i = K_i \quad \forall i \\ & \sum_{i=1}^{P}\mathbf{z}_i = \mathbf{1}_N \\ & 0 \le \mathbf{z_i} \le 1 \quad \forall i. \end{aligned} \quad (17)$$

It should be highlighted that SCP is a local heuristic and thus the final solution is dependent on the initial subarray selection vectors $\mathbf{z}_i^{(0)}$, $\forall i$. Hence, we consider several initialization points $\mathbf{z}_i^{(0)}$, $\forall i$ for optimization (17) and select the solution that provides the maximum objective function value. We use the MATLAB embedded CVX software [37] to solve the optimization problem (17).

B. Cardinality as an Optimization Variable

In this section, we consider the cardinality of the antennas in each subarray as an optimization variable of the SINR maximization problem (17). Adding the numbers of sensors per subarray as an optimization variable maintains the convexity of the SCP optimization problem (17) and the reformulated problem can be written as

$$\begin{aligned} \max_{\substack{\mathbf{z}_1,\ldots,\mathbf{z}_P \\ K_1,\ldots,K_P}} \quad & \sum_{i=1}^{P}\log|\hat{\mathbf{C}}_{a,i}^H\mathcal{D}(\mathbf{z}_i)\hat{\mathbf{C}}_{a,i} + \mathbf{R}_i| - T_i \\ \text{s.t.} \quad & \mathbf{1}_N^T\mathbf{z}_i = K_i \quad \forall i \\ & \sum_{i=1}^{P}\mathbf{z}_i = \mathbf{1}_N \\ & 0 \le \mathbf{z_i} \le 1 \quad \forall i. \end{aligned} \quad (18)$$

In this case, the optimization does not only decide the location of the sparse subarrays sensors but also their number, i.e., K_i, $i = 1,\ldots,P$, based on the mission information and requirements. It should be highlighted that this method should be applied in cases where there is no minimum requirement regarding the performance of the system for each source, since the solution will allocate more antennas to a source with higher channel gain.

IV. OPTIMUM SUBARRAY DESIGN THROUGH SINR CONSTRAINED OPTIMIZATION

The common aperture dual or multitask receiver platforms must provide a sufficient gain to the incoming signal regardless of whether it represents communication or radar

data. This gain improves successful decoding of symbols for the former case and enhances probability of target detection for the latter case. Hence, in this section, our primary objective is to design an algorithm that maximizes the SINR for some sources subject to attaining a specific set of SINRs for the remaining sources. By setting the cardinality of the antennas as an optimization variable, the proposed scheme not only derives the optimum sparse subarray configurations but also the optimal number of antennas ($K_i, \forall i$) for each subarray.

Without loss of generality, we consider that there is a predefined SINR criterion γ_l^*, $l = 1, \ldots, L$ for the first L out of a total of P SOI. With a total of N antennas placed on a uniform linear grid, we may define the optimum sparse subarray design with SINR constraints as selecting the optimum sparse subarrays that constitute a ULA. Each subarray considers one source of interest and jointly maximizes the SINR_i performance toward $P - L$ sources where $i = L + 1, \ldots, P$, while attaining the SINR threshold γ_l^*, $l = 1, \ldots, L$ for the rest of the sources. To achieve this arrangement, we consider the following constrained-SINR maximization problem:

$$\begin{aligned} \max_{\substack{\mathbf{z}_1,\ldots,\mathbf{z}_P \\ K_1,\ldots,K_P}} \quad & \sum_{i=L+1}^{P} \text{SINR}_i \\ \text{s.t.} \quad & \text{SINR}_l \geq \gamma_l^*,\ l = 1, \ldots, L \\ & \mathbf{1}_N^T \mathbf{z_i} = K_i \quad \forall i \\ & \sum_{i=1}^{P} \mathbf{z}_i = \mathbf{1}_N \\ & \mathbf{z}_i \in \{0, 1\}^N \quad \forall i. \end{aligned} \tag{19}$$

The nonconcave objective function and SINR constraints and also the nonconvex binary selection constraints $\mathbf{z}_i \in \{0, 1\}^N$ render the optimization (19) nonconvex. Similarly to Section III, we relax the selection vector constraints to box constraints and we exploit first-order Taylor series approximation SCP to iteratively approximate the objective function and the SINR constraints. We derive the following approximated convex optimization problem:

$$\begin{aligned} \max_{\substack{\mathbf{z}_1,\ldots,\mathbf{z}_P \\ K_1,\ldots,K_P}} \quad & \sum_{i=L+1}^{P} \log|\hat{\mathbf{C}}_{a,i}^H \mathcal{D}(\mathbf{z}_i)\hat{\mathbf{C}}_{a,i} + \mathbf{R}_i| - T_i \\ \text{s.t.} \quad & \log|\hat{\mathbf{C}}_{a,l}^H \mathcal{D}(\mathbf{z}_l)\hat{\mathbf{C}}_{a,l} + \mathbf{R}_l| - T_l \geq \gamma_l^*,\ l = 1, \ldots, L \\ & \mathbf{1}_N^T \mathbf{z}_i = K_i \quad \forall i \\ & \sum_{i=1}^{P} \mathbf{z}_i = \mathbf{1}_N \\ & 0 \leq \mathbf{z_i} \leq 1 \quad \forall i. \end{aligned} \tag{20}$$

The optimization (20) is a local heuristic problem and its solution depends on the initialization vectors $\mathbf{z}_i^{(0)}$. Hence, we initialize the SCP algorithm (20) with several starting points $\mathbf{z}_i^{(0)}$ and save the solution that gives the maximum objective function value.

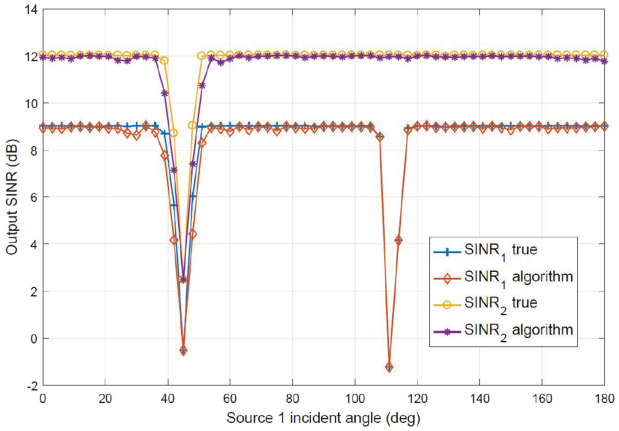

Fig. 2. Output SINR for subarrays 1 and 2 derived from enumeration and (17).

V. SIMULATION RESULTS

In this section, simulation results are presented to validate the effectiveness of the proposed joint aperture optimum subarray design algorithms.

A. Example 1

We consider a ULA consisting of $N = 16$ antennas with an interelement spacing of $d = \lambda/2$. The receiving platform aims to maximize the SINR of two separate sources utilizing two sparse subarrays of fixed number of antennas, $K_1 = K_2 = 8$. The first source signal arrives at the array from a direction $\phi_{s,1}$ that is changing from 0° to 180° with a step of 3°, and with an SNR set at 0 dB, whereas the second source is fixed at $\phi_{s,2} = 45°$, with an SNR of 3 dB. An interfering source is also active, impinging on the ULA from $\phi_{i,1} = 112°$ with an INR set at 20 dB. For each arrival angle of source 1, we obtain the corresponding optimum sparse subarrays regarding both sources according to SINR maximization (17), and using 12 random initialization points $\mathbf{z}_i^{(0)}$. In order to validate the efficiency of the first-order Taylor series approximation SCP, we obtain the true optimum sparse subarrays through enumeration and compare the output SINRs of both methods in Fig. 2. It is evident that the optimum performance of the proposed method closely approximates the global optimum solution obtained from enumeration. Moreover, there is an evident SINR drop for both subarrays when the two sources are closely separated, since each source, in essence, plays the role of an interfering signal for the reception of the other source. Subarray 1 experiences one more SINR drop when source 1 is closely located to the interfering source, whereas this drop is not present for subarray 2, since source 2 is fixed at $\phi_{s,2} = 45°$. In order to demonstrate the impact of the subarray configuration on the output SINR, we fix the incoming angle of source 1 at $\phi_{s,1} = 143°$ and enumerate all possible 12 870 subarray selections. We present the corresponding output SINR in descending values for both sources in Fig. 3. The cardinalities of all possible selections for subarrays 1 and 2 are obtained from $\frac{N!}{K_1!(N-K_1)!}$ and $\frac{N!}{K_2!(N-K_2)!}$, respectively, which are equal, since $N = K_1 + K_2$. It is clear that

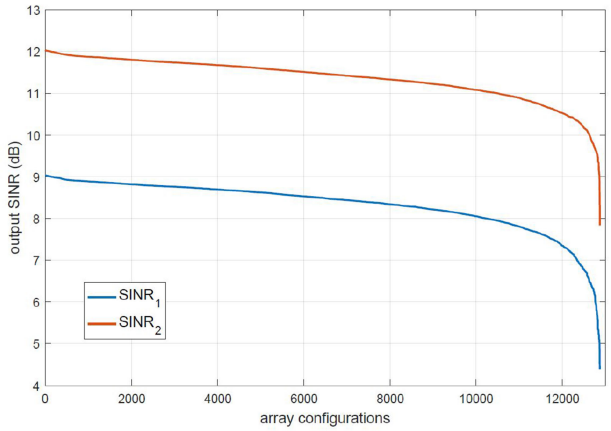

Fig. 3. Output SINR for all different sparse subarrays for $\phi_{s,1} = 143^\circ$ and $\phi_{s,2} = 45^\circ$.

TABLE I
Maximum SINR for Optimization (17) With Varying Number of Initialization Points $\mathbf{z}_i^{(0)}$ (dB)

Number of $\mathbf{z}_i^{(0)}$	SINR_1	SINR_2
2	8.9851	11.9685
4	8.9851	11.9728
6	8.9928	11.9728
8	9.0024	12.0134
10	9.0118	12.0188
12	9.0216	12.0242
14	9.0216	12.0242
16	9.0216	12.0242

the different subarray designs significantly alters the output SINR, up to 5 dB difference. As mentioned in Section III, the number of initialization points $\mathbf{z}_i^{(0)}$ affects the performance of the optimization (17). Table I presents the output SINR for subarrays 1 and 2 for different number of initialization vectors $\mathbf{z}_i^{(0)}$. It is evident that there is a minor increase in performance with increased number of initialization points. It also shows that even by using few initialization points, we achieve performance that closely approximates the global optimum, which is $\text{SINR}_1^* = 9.0306$ and $\text{SINR}_2^* = 12.0302$. Simulations also showed that there is insignificant change in SINR when using more than 12 initialization points.[1]

[1]Regarding the computational complexity of the proposed algorithm, it is noted that the complexity of an $N \times N$ matrix inversion is of the order $O(N^3)$ and the solution of a convex problem is of polynomial time complexity. In the proposed algorithm, we perform $m_{\text{iter}} \times n_{\text{iter}}$ iterations, where m_{iter} is the number of initialization points of the respective optimization and n_{iter} is the number of iterations needed to achieve the required Taylor approximation accuracy. During each iteration, P matrix inversions and P convex optimizations are performed, where P is the number of desired sources considered.

B. Example 2

In the next simulation, we extend the ULA to $N = 36$ antennas and add a third source of interest at $\phi_{s,3} = 68^\circ$ with SNR fixed for all sources at 0 dB. The interfering source is assumed to be the same as in the first example. We assume two cases of highly and weakly spatially correlated sources. Case I represents highly spatially correlated sources, where the incident angles of sources 1 and 2 are set at $\phi_{s,1} = 47^\circ$ and $\phi_{s,2} = 45^\circ$, respectively. In case II of low spatial correlation, the angles-of-arrival are set at $\phi_{s,1} = 143^\circ$ and $\phi_{s,2} = 45^\circ$, respectively. The spatial correlation matrices of the steering vectors corresponding to sources 1 and 2 for the high and the low correlation cases are

$$\mathbf{R}_{\text{high}} = \begin{bmatrix} 1 + 0j & 0.1318 + 0.6837j \\ 0.1318 - 0.6837j & 1 + 0j \end{bmatrix},$$
$$\mathbf{R}_{\text{low}} = \begin{bmatrix} 1 + 0j & 0.0060 + 0.0118j \\ 0.0060 - 0.0118j & 1 + 0j \end{bmatrix}.$$

In order to shed light on the mechanism of joint subarray design, we derive the optimum subarrays for the two cases of given antennas cardinality and when the cardinality is a design parameter, which are associated with (17) and (18), respectively. We also obtain the optimal subarrays by maximizing the output SINR for each of the sources when considered separately through the following optimization:

$$\begin{aligned} \max_{\mathbf{z}} \quad & \text{SINR}_{oi} \\ \text{s.t.} \quad & \mathbf{1}_N^T \mathbf{z} = K \\ & 0 \le \mathbf{z} \le 1 \end{aligned} \tag{21}$$

for $i = 1, \ldots, P$. Optimization (21) is nonconvex and can be recasted as a convex one by using SCP. Since there is no explicit constraint on shared antennas across subarrays, some antennas could be allocated to more than one subarray and hence this design cannot be used for simultaneous multitask function. The subarray configurations derived from (17), (18), and (21) are depicted in Figs. 4 and 5 for the highly and the weakly correlated cases, respectively. In particular, the blue dots represent the respective active sensors for the corresponding subarray. Two important observations are in order: First, for the case of highly spatially correlated sources, the optimum subarrays for sources 1 and 2 obtained from the separate design (21) are fully overlapped [see Fig. 4(g) and (h)], since they consist of exactly the same antennas, whereas for the weakly correlated case they share only 4 out of 12 antennas [see Fig. 5(d) and (e)]. Hence, the competition for the optimum antennas located at the two far edges of the ULA in the joint aperture subarray design is more intense for higher spatial correlation of the SOI. As depicted in Fig. 4, subarrays 1 and 2 from (17) and (18) contest over the optimal antennas located at the two far edges of the ULA, whereas most of the antennas in the center of the ULA are allocated to subarray 3. The second observation is that the optimum subarray configurations from both (17) and (18) is exactly the

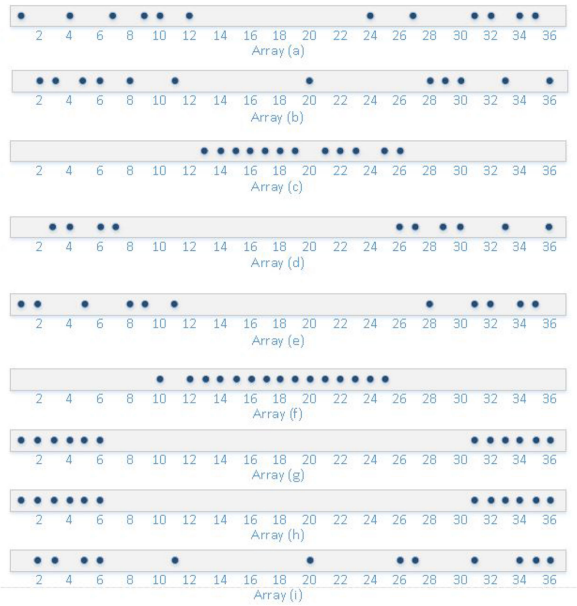

Fig. 4. Arrays for case I: (a) Subarray 1 for given cardinality of antennas (17), (b) Subarray 2 from (17), (c) Subarray 3 from (17), (d) Subarray 1 when the cardinality is a design parameter (18), (e) Subarray 2 from (18), (f) Subarray 3 from (18), (g) Subarray 1 from separate design (21), (h) Subarray 2 from (21), and (i) Subarray 3 from (21).

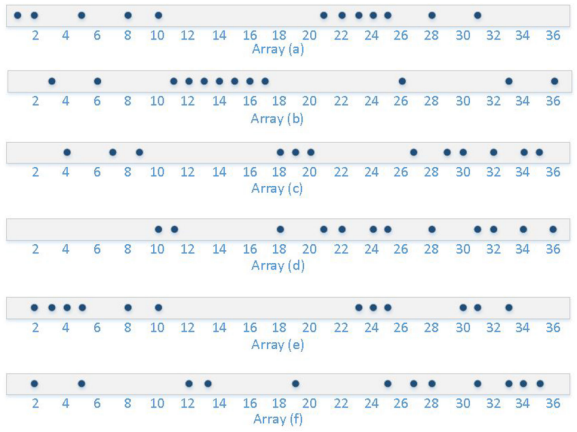

Fig. 5. Arrays for case II: (a) Subarray 1 for given cardinality of antennas (17) and when the cardinality is a design parameter (18), (b) Subarray 2 from (17) and (18), (c) Subarray 3 from (17) and (18), (d) Subarray 1 from (21), (e) Subarray 2 from (21), and (f) Subarray 3 from (21).

same for the weakly correlated sources, as seen in Fig. 5. However, for the case of highly correlated sources, optimization (18) allocates more antennas to the less correlated source 3 ($K_1 = 10$, $K_2 = 11$, $K_3 = 15$), since it results in higher total SINR for the system, as shown in Table II. This table presents the maximum output SINR values and the total SINR for all three sources for optimizations (17), (18), and (21). It is also evident from Table II that for the case of highly correlated sources, the proposed methods provide a substantially lower SINR as compared to separate subarray optimization. On the other hand, for less correlated sources, the joint optimizations (17) and (18) provide almost

TABLE II
Maximum SINR for the Proposed Methods of (17), (18) and Separate Optimization (21) (dB)

	Eq.(17)	Eq.(18)	Eq.(21)
$SINR_1$, Case I	9.1294	8.5465	10.1743
$SINR_2$, Case I	9.1989	9.2434	10.1698
$SINR_3$, Case I	10.7389	11.7027	10.7529
total SINR, Case I	29.0672	29.4926	31.097
$SINR_1$, Case II	10.7434	10.7434	10.7435
$SINR_2$, Case II	10.6530	10.6530	10.7537
$SINR_3$, Case II	10.6844	10.6844	10.7547
total SINR, Case II	32.0808	32.0808	32.2519

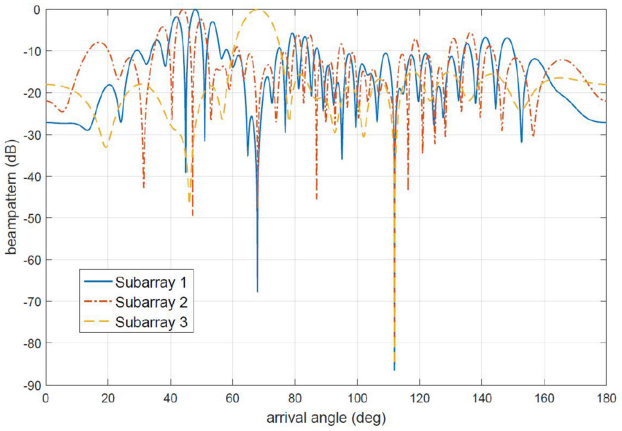

Fig. 6. Beampatterns for all subarrays for case I from (17).

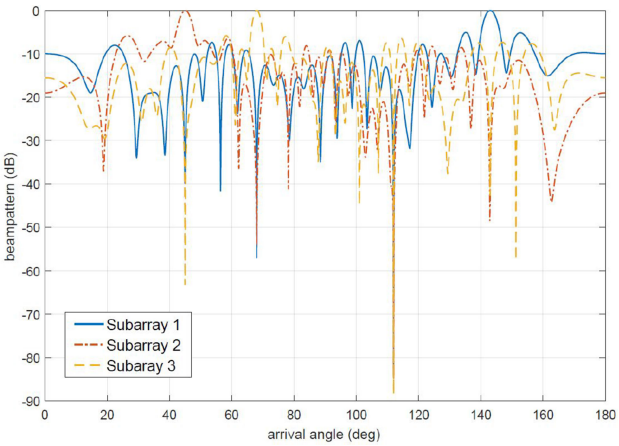

Fig. 7. Beampatterns for all subarrays for case II from (17).

identical performance to the separate design technique (21). The beampatterns for the optimum subarrays obtained from (17) for the highly and weakly correlated cases are plotted in Figs. 6 and 7, respectively.

C. Example 3

In this simulation, we consider the same layout as the weak correlation case of the previous example. We assume

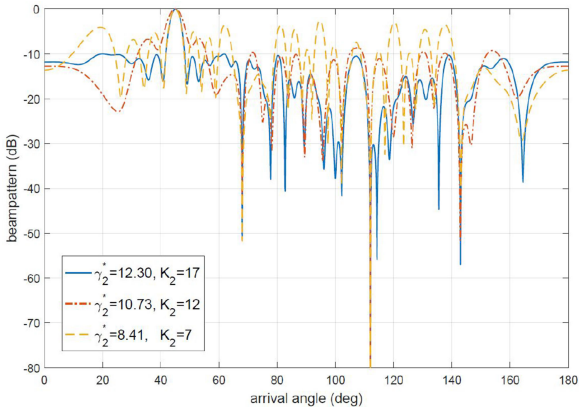

Fig. 8. Beampatterns toward source 2 for different γ_2^*.

TABLE III
Optimal Number of Antennas for Subarays 1, 2, and 3 and Maximum SINR_1 and SINR_3 (dB) for Different Target SINR γ_2^*

$SINR_2$ target	K_1	K_2	K_3	$SINR_1$	$SINR_3$
$\gamma_2^* = 8.41$	14	7	15	11.38	11.73
$\gamma_2^* = 10.73$	12	12	12	10.77	10.75
$\gamma_2^* = 12.30$	10	17	9	9.88	9.45

a predefined fixed desired SINR_2 for source 2. The primary objective is to obtain three separate sparse subarrays that constitute the entire ULA and maximize the SINR at the output of subarrays 1 and 3 while satisfying the desired output SINR for subarray 2. It is noted that the algorithm decides on both the optimal locations of the antennas for each subarray and also the optimal number of antennas for each subarray (K_1, K_2, K_3). The beampatterns toward source 2 for different SINR thresholds γ_2^* are shown in Fig. 8. It is evident that higher γ_2^* generates a more accurate mainbeam toward source 2 with lower sidelobe levels and more efficient mitigation of interference. The optimum cardinality of the antennas in each subarray along with the maximum SINRs obtained from (20) for different γ_2^* are listed in Table III. As expected, the higher the desired SINR level toward source 2 is, the more antennas are allocated to subarray 2, which naturally leads to a drop of SINR for the other subarrays.

D. Example 4

In order to further demonstrate the superiority of the proposed adaptive algorithms, we compare the performance of the sparse subarrays obtained from (17) to the case when the structured nested and coprime arrays are utilized to derive subarray 1 [38], [39]. We consider a ULA of $N = 20$ antennas and two SOI. For a fair comparison, we employ $K_1 = 8$ antennas to design the optimum adaptive sparse subarray 1 from (17) and also eight antennas to build the prefixed nested and coprime subarray 1. The angles-of-arrival of the SOI are $\phi_{s,1} = 80^\circ$ and $\phi_{s,2} = 68^\circ$ with their SNR set at 0 dB. An interfering source is also present at $\phi_{i,1} = 112^\circ$ with INR = 20 dB. The subarray 1 structures

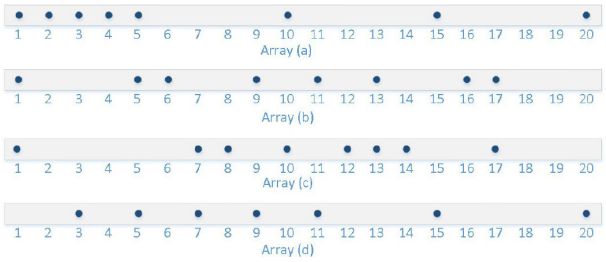

Fig. 9. Subarray 1: (a) proposed method (17), (b) Nested array, (c) Coprime array, (d) proposed method (20) with $\gamma_1^* = 8.4102$.

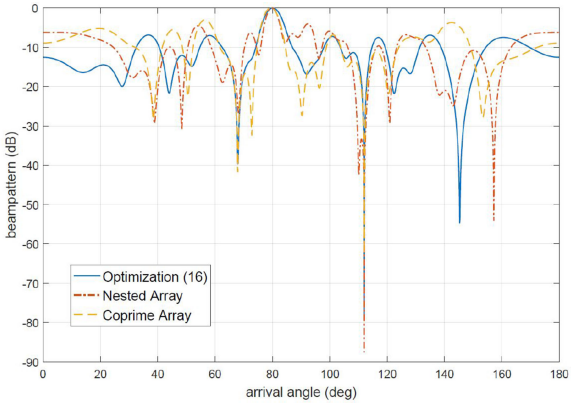

Fig. 10. Beampatterns for subarrays (a), (b), and (c) in Fig. 9.

TABLE IV
Comparison of the System Performance for the Proposed Methods, the Nested Arrays, and the Coprime Arrays Schemes

	K_1	K_2	$SINR_1$	$SINR_2$
Optimization (17)	8	12	8.9639	13.7877
Nested	8	12	8.4102	13.3058
Coprime	8	12	7.9412	13.4557
Optimization (20), $\gamma_1^* = 8.4102$	7	13	8.4102	14.1116

are depicted in Fig. 9 and the corresponding beampatterns in Fig. 10. It can be observed that the proposed joint sparse subarray design yields a better shaped beampattern with deeper nulls at the direction of interference and lower sidelobes when contrasted with the prefixed nested and coprime arrays beampattern. In order to quantify the comparison, Table IV shows the maximum SINR obtained from the proposed adaptive algorithms and the prefixed techniques. We also added the optimum subarray structure obtained from (20) with $\gamma_1^* = 8.4102$ (subarray (d) in Fig. 9) to match the SINR performance of the prefixed nested array technique. It is evident that the proposed adaptive algorithms substantially outperform the prefixed nested and coprime schemes in terms of output SINR for the SOI. Furthermore, as shown in Table IV, the proposed adaptive optimization (20) matches the performance of the nested arrays structure toward source 1, even though employing only seven antennas. Therefore, the extra antenna can be allocated to subarray 2, maximizing the SINR_2 performance for source 2 as shown in Table IV.

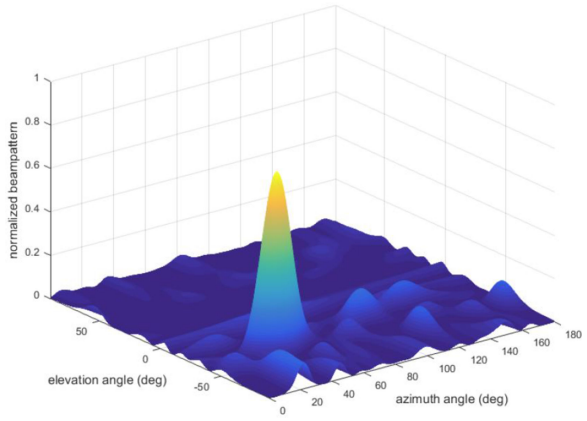

Fig. 11. Normalized beampattern of subarray 1.

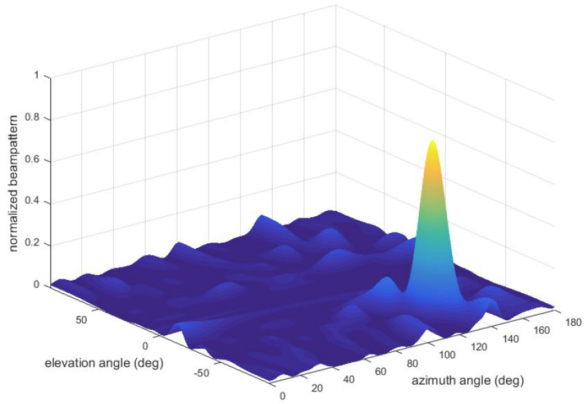

Fig. 12. Normalized beampattern of subarray 2.

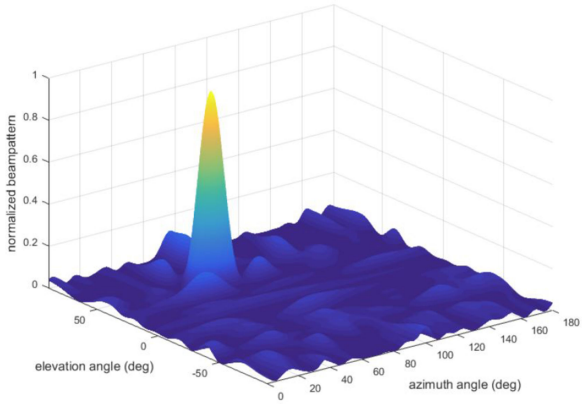

Fig. 13. Normalized beampattern of subarray 3.

E. Example 5

The proposed sparse subarray design algorithms can be also applied in the case of planar antenna arrays. For illustration, we consider a 10×10 uniform rectangular array with an interelement spacing among any two adjacent antennas along any column or row is $d_x = d_y = \lambda/2$, respectively. Three SOI are considered with angles of arrival $\theta_{s,1} = -35^\circ$, $\theta_{s,2} = -55^\circ$, $\theta_{s,3} = 45^\circ$, where $\theta_{s,i}$ denotes the elevation angle of source i and $\hat{\phi}_{s,1} = 47^\circ$, $\hat{\phi}_{s,2} = 130^\circ$, $\hat{\phi}_{s,3} = 68^\circ$, with $\hat{\phi}_{s,i}$ stands for the azimuth angle of source i. There is also one interfering source present impinging on the two-dimensional array from $\theta_{i,1} = 74^\circ$ (elevation), $\hat{\phi}_{i,1} = 112^\circ$ (azimuth). We allocate 34 antennas for subarray 3 and 33 antennas for each of the subarrays 1 and 2, i.e., $K_3 = 34$, $K_1 = K_2 = 33$. The respective normalized beampatterns for each subarray are plotted in Figs. 11, 12, and 13. The sparse separated subarrays configuration is shown in Fig. 14 and the collective contour plot of all three beampatterns is depicted in Fig. 15.

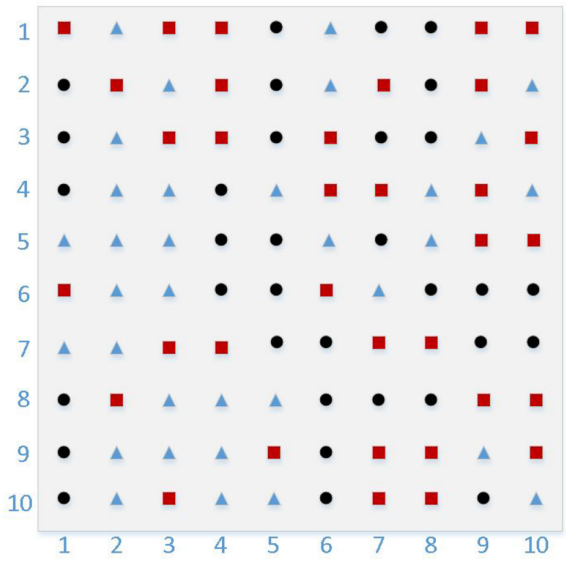

Fig. 14. Sparse subarrays configuration map: circle: subarray 1, triangle: subarray 2, square: subarray 3.

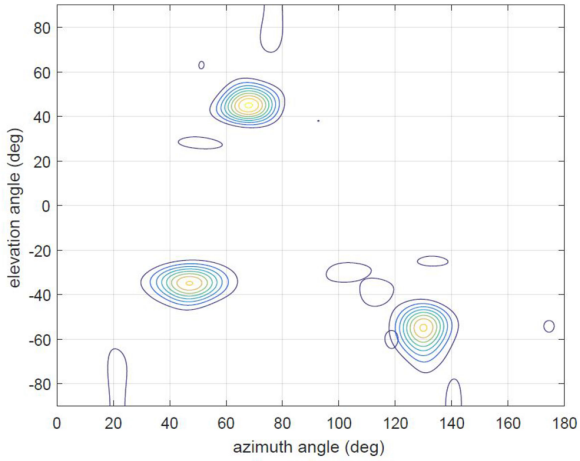

Fig. 15. Collective contour plot of the three beampatterns.

VI. CONCLUSION

We have examined the problem of sparse array design, where the array aperture is divided among different subarrays—a concept known as shared aperture. At first, we proposed an algorithm that optimally decides the locations of predetermined number of antennas for each subarray using SINR as a criterion and conditioned of having unshared antennas among the subarrays. Furthermore, we generalized the above problem by including the cardinality of the antennas in each subarray as an optimization variable,

providing more degrees of freedom to the algorithm to further increase the efficiency of the system. Additionally, we proposed an algorithm that maximizes the SINR for some sources, while satisfying a certain SINR threshold for the other sources. SCP and Taylor series approximation techniques were employed to render the initially nonconvex sparse subarray design as a convex problem. Simulation results demonstrated that the proposed method closely approximates the true optimum sparse subarray design performance obtained by enumeration. Furthermore, it was shown that the proposed algorithm can be applied to high spatially correlated sources and in the case of planar antenna arrays. Finally, the superior performance of the resulting subarrays over other prefixed sparse array configurations was also demonstrated.

REFERENCES

[1] D. M. Pozar and S. D. Targonski
A shared-aperture dual-band dual-polarized microstrip array
IEEE Trans. Antennas Propag., vol. 49, no. 2, pp. 150–157, Feb. 2001.

[2] G. C. Tavik *et al.*
The advanced multifunction RF concept
IEEE Trans. Microwave Theory Techn., vol. 53, no. 3, pp. 1009–1019, Mar. 2005.

[3] G. Kwon, J. Y. Park, D. H. Kim, and K. C. Hwang
Optimization of a shared-aperture dual-band transmitting/receiving array antenna for radar applications
IEEE Trans. Antennas Propag., vol. 65, no. 12, pp. 7038–7051, Dec. 2017.

[4] I. E. Lager, C. Trampuz, M. Simeoni, C. I. Coman, and L. P. Ligthart
Application of the shared aperture antenna concept to radar front-ends : advantages and limitations
In *Proc. 4th Eur. Conf. Antennas Propag.*, 2010, pp. 1–4.

[5] G. Oliveri, F. Viani, and A. Massa
Synthesis of linear multi-beam arrays through hierarchical almost difference set-based interleaving
IET Microw., Antennas Propag., vol. 8, no. 10, pp. 794–808, 2014.

[6] A. Hassanien, M. W. Morency, A. Khabbazibasmenj, S. A. Vorobyov, J.-Y. Park, and S.-J. Kim
Two-dimensional transmit beamforming for MIMO radar with sparse symmetric arrays
In *Proc. IEEE Radar Conf.*, 2013, pp. 1–6.

[7] X. Shen and P. K. Varshney
Sensor selection based on generalized information gain for target tracking in large sensor networks
IEEE Trans. Signal Process., vol. 62, no. 2, pp. 363–375, Jan. 2015.

[8] M. G. Amin, X. Wang, Y. D. Zhang, F. Ahmad, and E. Aboutanios
Sparse arrays and sampling for interference mitigation and DOA estimation in GNSS
Proc. IEEE, vol. 104, no. 6, pp. 1302–1317, Jun. 2016.

[9] X. Wang, E. Aboutanios, and M. G. Amin
Adaptive array thinning for enhanced DOA estimation
IEEE Signal Process. Letters, vol. 22, no. 7, pp. 799–803, Jul. 2015.

[10] H. C. Lin
Spatial correlations in adaptive arrays
IEEE Trans. Antennas Propag., vol. 30, no. 2, pp. 212–223, Mar. 1982.

[11] O. Mehanna, N. Sidiropoulos, and G. Giannakis
Joint multicast beamforming and antenna selection
IEEE Trans. Signal Process., vol. 61, no. 10, pp. 2660–2674, May 2013.

[12] S. Applebaum
Adaptive arrays
IEEE Trans. Antennas Propag., vol. AP-24, no. 5, pp. 585–598, Sep. 1976.

[13] B. Widrow, P. E. Mantey, L. J. Griffiths, and B. B. Goode
Adaptive antenna systems
Proc. IEEE, vol. 55, no. 12, pp. 2143–2159, Dec. 1967.

[14] K. Buckley and L. Griffiths
An adaptive generalized sidelobe canceller with derivative constraints
IEEE Trans. Antennas Propag., vol. AP-34, no. 3, pp. 311–319, Mar. 1986.

[15] A. Deligiannis, S. Lambotharan, and J. A. Chambers
Beamforming for fully-overlapped two-dimensional Phased-MIMO radar
In *Proc. IEEE Radar Conf.*, Arlington, VA, USA, 2015, pp. 0599–0604.

[16] A. Deligiannis, S. Lambotharan, and J. A. Chambers
Game theoretic analysis for MIMO radars with multiple targets
IEEE Trans. Aerosp. Electron. Syst., vol. 52, no. 6, pp. 2760–2774, Dec. 2016.

[17] L. E. Brennan and L. S. Reed
Theory of adaptive radar
IEEE Trans. Aerosp. Electron. Syst., vol. AES-9, no. 2, pp. 237–252, Mar. 1973.

[18] R. Compton
An adaptive array in a spread-spectrum communication system
Proc. IEEE, vol. 66, no. 3, pp. 289–298, Mar. 1978.

[19] P. Napier, A. Thompson, and R. Ekers
The very large Array: Design and performance of a modern synthesize radio telescope
Proc. IEEE, vol. 71, no. 11, pp. 1295–1320, Nov. 1983.

[20] P. E. Dewdney, P. J. Hall, R. T. Schilizzi, and T. J. L. W. Lazio
The square kilometre array
Proc. IEEE, vol. 97, no. 8, pp. 1482–1496, Aug. 2009.

[21] D. H. Johnson and S. R. Degraaf
Improving the resolution of bearing in passive sonar arrays by eigenvalue analysis
IEEE Trans. Acoust., Speech, Signal Process., vol. 30, no. 4, pp. 638–647, Aug. 1982.

[22] A. F. Morabito, A. R. Lagana, G. Sorbello, and T. Isernia
Mask-constrained power synthesis of maximally sparse linear arrays through a compressive-sensing-driven strategy
J. Electromagn. Waves Appl., vol. 29, no. 10, pp. 1384–1396, 2015.

[23] R. L. Haupt
Phase-only adaptive nulling with a genetic algorithm
IEEE Trans. Antennas Propag., vol. 45, no. 6, pp. 1009–1015, Jun. 1997.

[24] L. Poli, P. Rocca, M. Salucci, and A. Massa
Reconfigurable thinning for the adaptive control of linear arrays
IEEE Trans. Antennas Propag., vol. 61, no. 10, pp. 5068–5077, Oct. 2013.

[25] O. T. Demir and T. E. Tuncer
Optimum discrete transmit beamformer design
Digital Signal Process., vol. 36, pp. 57–68, 2015.

[26] X. Wang, M. G. Amin, X. Wang, and X. Cao
Sparse array quiescent beamformer design combining adaptive and deterministic constraints
IEEE Trans. Antennas Propag., vol. 65, no. 11, pp. 5808–5818, Nov. 2017.

[27] J. Capon
High-resolution frequency-wavenumber spectrum analysis
Proc. IEEE, vol. 57, no. 8, pp. 1408–1418, Aug. 1969.

[28] X. Wang, M. Amin, and X. Cao
Analysis and design of optimum sparse array configurations for adaptive beamforming
IEEE Trans. Signal Process., vol. 66, no. 2, pp. 340–351, Jan. 2017.

[29] S. M. Kay
Fundamentals of Statistical Signal Processing: Detection Theory. Englewood Cliffs, NJ, USA: Prentice-Hall, 1998.

[30] F. Rashid-farrokhi, K. J. R. Liu, S. Member, and L. Tassiulas
Transmit beamforming and power control for cellular wireless systems
IEEE J. Sel. Areas Commun., vol. 16, no. 8, pp. 1437–1450, Oct. 1998.

[31] H. L. Van Trees
Detection, Estimation, and Modulation Theory, Optimum Array Processing. New York, NY, USA: Wiley, 2004.

[32] A. Deligiannis, A. Panoui, S. Lambotharan, and J. Chambers
Game-Theoretic power allocation and the nash equilibrium analysis for a multistatic MIMO radar network
IEEE Trans. Signal Process., vol. 65, no. 24, pp. 6397–6408, Dec. 2017.

[33] X. Wang, E. Aboutanios, and M. G. Amin
Slow radar target detection in heterogeneous clutter using thinned space-time adaptive processing
IET Radar, Sonar Navig., vol. 10, no. 4, pp. 726–734, 2016.

[34] H. Tuy
Convex Analysis and Global Optimization. New York, NY, USA: Springer, 1998.

[35] R. Horst
Introduction to Global Optimization. New York, NY, USA: Springer, 2000.

[36] S. Boyd and L. Vandenberghe
Convex Optimization. Cambridge, U.K.: Cambridge Univ. Press, 2004, 2004.

[37] M. Grant, S. Boyd, and Y. Ye
CVX: Matlab Software for Disciplined Convex Programming, 2008.

[38] P. Pal and P. P. Vaidyanathan
Nested arrays: A novel approach to array processing with enhanced degrees of freedom
IEEE Trans. Signal Process., vol. 58, no. 8, pp. 4167–4181, Aug. 2010.

[39] M. G. Amin, P. P. Vaidyanathan, Y. D. Zhang, and P. Pal
Special issue on coprime sampling and arrays
Digital Signal Process., vol. 61, pp. 1–96, 2017.

Anastasios Deligiannis (S'13–M'16) received the Diploma degree (Bachelor and Masters degrees equivalent) from the School of Electrical and Computer Engineering, University of Patras, Patras, Greece, in 2012. He received the Ph.D. degree in radar signal processing from Loughborough University, Loughborough, U.K., in 2016.

Since June 2016, he has been a Research Associate in signal processing with Loughborough University. His research focuses on signal processing algorithms, sparse array design, convex optimization and game theoretic methods, within the radar network framework and wireless communications.

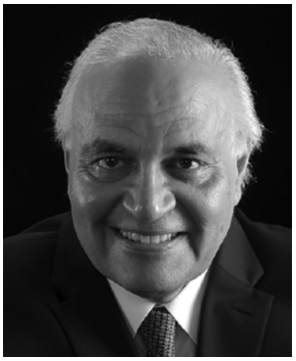

Moeness Amin (F'01) received the B.Sc. degree from the Faculty of Engineering, Cairo University, Giza, Egypt, in 1976, the M.Sc. degree from the University of Petroleum and Minerals, Saudi Arabia, in 1980, and the Ph.D. degree in electrical engineering from the University of Colorado, Boulder, CO, USA, in 1984.

Since 1985, he has been with the Faculty of the Department of Electrical and Computer Engineering, Villanova University, Villanova, PA, USA, where he became the Director of the Center for Advanced Communications, College of Engineering, in 2002. He has more than 800 journal and conference publications in signal processing theory and applications, covering the areas of wireless communications, radar, sonar, satellite navigations, ultrasound, healthcare, and RFID. He has coauthored 21 book chapters and is the Editor of three books titled: *Through the Wall Radar Imaging* (CRC Press, 2011), *Compressive Sensing for Urban Radar* (CRC Press, 2014), and *Radar for Indoor Monitoring* (CRC Press, 2017).

Dr. Amin is a Fellow of the International Society of Optical Engineering; Fellow of the Institute of Engineering and Technology; and a Fellow of the European Association for Signal Processing. He is the Recipient of the 2017 Fulbright Distinguished Chair in Advanced Science and Technology; Recipient of the 2016 Alexander von Humboldt Research Award; Recipient of the 2016 IET Achievement Medal; Recipient of the 2014 IEEE Signal Processing Society Technical Achievement Award; Recipient of the 2010 NATO Scientific Achievement Award; Recipient of the 2009 Individual Technical Achievement Award from the European Association for Signal Processing; Recipient of the 2015 IEEE Aerospace and Electronic Systems Society Warren D White Award for Excellence in Radar Engineering; and Recipient of the 2010 Chief of Naval Research Challenge Award. He is the Recipient of the IEEE Third Millennium Medal. He was a Distinguished Lecturer of the IEEE Signal Processing Society, 2003–2004, and is the past Chair of the Electrical Cluster of the Franklin Institute Committee on Science and the Arts.

Sangarapillai Lambotharan (SM'06) received the Ph.D. degree in signal processing from Imperial College London, London, U.K., in 1997.

He is a Professor of Digital Communications and the Head of Signal Processing and Networks Research Group, Wolfson School Mechanical, Electrical and Manufacturing Engineering, Loughborough University, Loughborough, U.K. He remained with Imperial College London until 1999 as a Postdoctoral Research Associate. He was a visiting Scientist with the Engineering and Theory Centre, Cornell University, Ithaca, NY, USA, in 1996. Between 1999 and 2002, he was with Motorola Applied Research Group, U.K. and investigated various projects including physical link layer modeling and performance characterization of GPRS, EGPRS, and UTRAN. He was with King's College London and Cardiff University as a Lecturer and a Senior Lecturer, respectively, from 2002 to 2007. His current research interests include 5G networks, MIMO, radars, smart grids, machine learning, network security and convex optimizations, and game theory. He has published more than 200 technical journal and conference articles in these areas.

Giuseppe (Joe) Fabrizio (F'16) received the Bachelor's of Engineering and Ph.D. degrees from the School of Electrical and Electronic Engineering, University of Adelaide, Adelaide, SA, Australia, in 1992 and 2000.

He joined Australia's Defence Science and Technology (DST) Group in 1993, working in the Signal Processing Group of the High Frequency Radar Division. From 2004 to 2015, he led the Radar Signal Processing and Electronic Warfare section, with the primary responsibility to implement adaptive processing techniques and practical EW solutions to enhance the operational performance of the Jindalee Operational Radar Network (JORN). In 2015, he was appointed Group Leader—Microwave Radar Systems in DST, where he currently leads research and development in active electronically scanned array (AESA) radar systems and delivers radar related S&T advice to Defence. He is the principal author of more than 60 peer-reviewed journal and conference publications. He has collaborated with international Defence S&T organizations under Memorandum of Understanding agreements and has contributed to several NATO SET panels and TTCP task group activities. He has actively led collaborations with partners in industry and academia to produce S&T outcomes for Defence work programs. He has interest in research and development of next-generation broadband AESA technology for multifunction RF Systems that simultaneously support advanced radar, electronic warfare and communications.

Dr. Fabrizio received the prestigious IEEE Barry Carlton Award for the best paper published in the Transactions on Aerospace and Electronic Systems (AES) in 2003 and 2004. He was granted the DST Science and Engineering Excellence Award in 2007 for contributions to robust adaptive beamforming in JORN. In the same year, he received a Defence Science Fellowship to pursue collaborative R&D at La Sapienza University, Rome, Italy. He was selected as the recipient of the 2011 IEEE Fred Nathanson Memorial Radar Award for technical contributions to OTHR and Radar Signal Processing. He is the author of *Over-the-Horizon Radar - Fundamental Principles, Signal Processing and Practical Applications* (McGraw-Hill, 2013). He has been a member of the IEEE AES International Radar Systems Panel since 2008 and an IEEE AES Society Distinguished Lecturer since 2015. He served as the Vice President of Education on the IEEE AES Society Board of Governors (2012–2015) and is currently the President of the IEEE AES Society (2018–2019).